ATLAS Finger: a Prosthetic Finger Mechanism for Robotic applications

Article · July 2023

2 authors:

Aryan Gorjestani
Islamic Azad University, Pardis Branch
1 PUBLICATION **0** CITATIONS
SEE PROFILE

Farzad Cheraghpour Samavati
Islamic Azad University, Pardis Science and Technology Branch
49 PUBLICATIONS **190** CITATIONS
SEE PROFILE

INTERNATIONAL JOURNAL OF ROBOTICS
(THEORY AND APPLICATIONS)
E-mail: IJR@kntu.ac.ir

ATLAS Finger: a Prosthetic Finger Mechanism for Robotic applications

A. Gorjestani [a] and F. Cheraghpour Samavati [b,1]

[a] Intelligent Mechanical Systems Research Lab, Department of Mechanical Engineering, Pardis Science & Technology Branch, Islamic Azad University, Tehran, Iran
[b] Department of Mechanical Engineering, Pardis Science & Technology Branch, Islamic Azad University, Tehran, Iran

ARTICLE INFO

Article history:
Submit: 2021-09-05
Revise: 2023-05-13
Accept: 2023-07-10

Keywords:
Prosthetic Finger
Artificial Finger
3D Print
Finger Mechanism
Upper limb amputation
Linkage-driven prosthesis

ABSTRACT

The first and most important part of Mechanical design of a prosthetic hand is the finger. Over the years, many diverse and innovative designs for the prosthetic finger mechanism have been proposed. For this aim, capability of grasping objects in a stable manner with suitable contact force and an anthropomorphic structure are critical factors for design. In this article, after examining the anatomy of a natural finger the most prominent mechanisms offered by researchers are investigated. Then the ATLAS artificial finger mechanism and the 3D-printed prototype of which is introduced. Finally, the amount of contact force produced by the ATLAS upper finger phalange is calculated and verified with some motion study simulations. For validation of proposed mechanism, the amount of contact forces produced by the designed finger and the natural finger are compared. The results prove the effectiveness of the design.

[1] Corresponding address: Pardis Science & Technology Branch, Islamic Azad University, Tehran, Iran
Tel.: +98 2176281010; fax: +982176281213.
E-mail address: samavati@pardisiau.ac.ir.

1. Introduction

Human hand health has always been exposed to risk factors such as car accidents, chainsaws, infectious diseases, tumors, etc., [1] Sometimes these factors cause the amputation of one or more fingers, claws, forearms or even an arm in a person. In the past, they tried to eliminate these shortcomings by making artificial limbs made of wood or metal. But with the advancement of engineering, robots were designed that could act much like a natural hand. Using these robots, these people can largely eliminate their mobility defects and go about their daily lives like a healthy human being. The field of robotic end effector (EE) design and the field of lower arm prosthesis design have many parallels. However, the requirements for designing a manipulator for applied by a robot are different than those for use by an amputee. In particular, size, weight, power consumption, and beautifying appearance are of greater importance when designing prosthesis.

The hand is one of the most functional limbs of the human body which has capability to perform a variety of tasks. During hand movement, the tissues around the related joints will be deformed, including skin, muscles, tendons, fascia, joint capsules, and ligaments. The movement of the fingers of a human hand begins with a cerebral command. These commands are transmitted by nerve fibers throughout the body and reach the muscles of the knuckles. As the muscles expand and contract, the knuckles move around the joints. Every human finger has four bones (phalanges) and three joints. *Metacarpal* bones make up the palm. The first finger phalange is the *Proximal*, which is attached to the palmar bones by the *Metacarpal Phalange* (MCP) joint. There is a *Proximal and Intermediate Phalange* (PIP) joint between the Proximal and Intermediate and a *Distal and Intermediate Phalange* (DIP) joint between the Intermediate and Distal. Unlike the four fingers Index, Middle, Ring, and Little, the thumb does not have an Intermediate phalange, and the joint name between the Proximal and Distal phalange is IP. **Fig. 1.**

The closer it can be to a natural finger, the more valuable that design is. One of the most important features of a natural finger is Pre-Shaping motion, [2]. If the finger deforms before contact with the object, it has a Pre-Shaping motion feature. With grasp planning point of view, there are two relevant features of reach-to-grasp actions. The first characteristic is that reach and grasp are implemented through two specialized visuo-motor channels that appear to be coordinated. The second characteristic is that aperture is scaled to object size and there is a linear relationship between maximum aperture and object diameter. Generally, artificial fingers that have only one phalange do not have Pre-Shaping motion feature, [3]. **Fig. 2.**

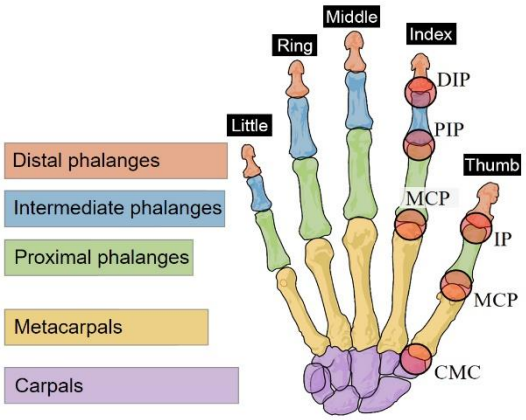

Fig. 1 Joints and phalanges of human hand, [4]

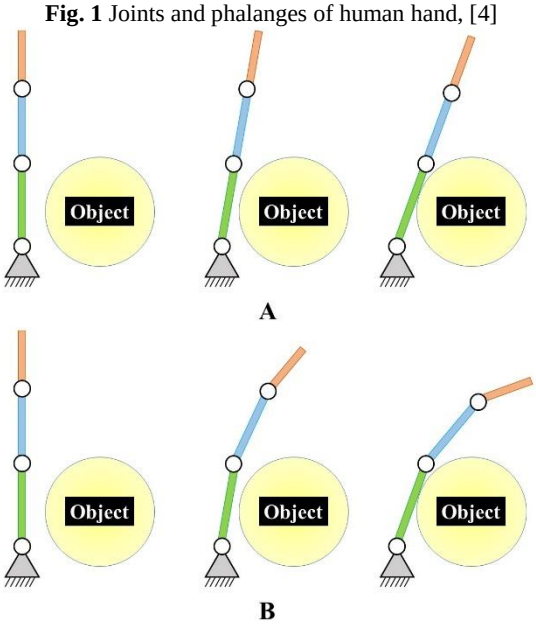

Fig. 2 Prosthetic finger without (A) and with (B) Pre-Shaping feature

Shape adaptability is another feature of the artificial finger, [2]. In this feature, when the proximal phalange hits the object and stops moving, the other phalanges continue to move until the finger loops around the object, [5]. **Fig. 3.**

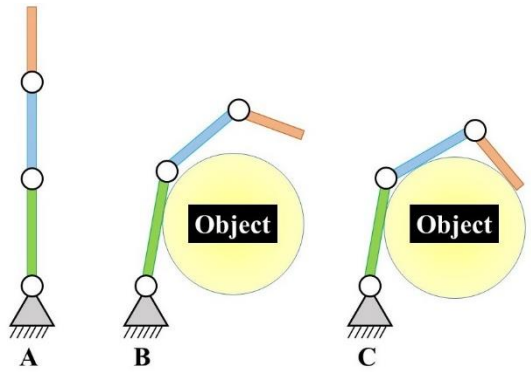

Fig. 3 Initial state (A), a prosthetic finger without (B) and with (C) shape adaptive motion

The last important feature of artificial fingers is pinching motion, [5]. When the index finger and thumb grip an object, the direction of rotation of the DIP joint of the index finger is reversed by rotating the other joint, causing the distal phalange to be in a different position from the other joints, [6]. **Fig. 4.**

Fig. 4 Pinching motion; rotation is CW in the PIP joint and CCW in the DIP.

Other features of artificial finger design include the force of contact of the joints with the body, stability, workspace, stiffness, weight, and compactness, [2, 5].

2. Prosthetic Finger Actuators

The first idea that comes to mind to move the artificial finger joints is to put a motor for each joint. Because each finger has 3 degrees of freedom (DOFs), 3 motors should be allocated to move it. But this will make the size and weight of the artificial finger much larger than the natural finger, which makes this idea seem such a poor design, [5].

In some designs, a motor called an under-actuated motor is used to move all five fingers, [7]. For example, the prosthetic fingers in the Yale *MyoAdapt* 3D-printed Hand, using a DC motor and a Whiffletree mechanism, open and close the fingers, [8]. The prosthetic fingers in Wattanasiri's design are opened and closed by a DC brushless motor with a linear mechanism, [9]. In Xu's design the finger actuated by a DC motor and the continuum differential mechanism, [10]. But the prosthetic fingers of *Michelangelo* are driven by two motors. One motor is used to move the four fingers and the MCP thumb joint and the other motor is used to move the IP joint of the thumb. The artificial fingers in the BeBionic hand are driven by 5 linear actuators and in the iLimb by 5 DC motors, which are considered to be under-actuated hands, since each of these hands has 6 degrees of freedom. [11].

Vincent's hand has 6 degrees of freedom and its fingers are driven by 6 DC motors. In Vincent, the thumb has two motors, one for the MCP joint and the other for the IP joint. This type of handle is called fully-actuated. [11]. In some other categories, such as Shadow hand, the number of motors exceeds the number of degrees of freedom, which is called over-actuated.

3. Prosthetic Finger Mechanisms

The movement mechanism of artificial fingers can be classified according to the method of movement. Some fingers use a tendon system to move, such as the *KNTH*, [12], *KNTU* hand, [13], the *Galileo* hand, [14]. Some other linkage-driven mechanisms are used, such as *BeBionic*, [11], and *LISA* hand, [15]. Some fingers also use a combination of these two methods; Like *Vincent*, [11].

Artificial fingers that move using the linkage-driven mechanism can be categorized based on the number of DOF of that mechanism, [5]. The mechanism of artificial fingers generally has between 1 to 3 DOFs. Rarely, fingers with 4 DOF have also been introduced, [5], [16]. Increasing the number of degrees of freedom due to weight and size is unreasonable, [5], [17]. On the other hand, because the natural finger has 3 DOF, increasing the DOF of the artificial finger is of little use, [5].

The *S-Finger* is a 1 DoF artificial finger with the Intermediate and Proximal phalange tightly connected, [18]. This finger has two joints, the MCP joint which is connected to the DC motor and the DIP joint which moves the distal phalange. The DIP joint is connected to the MCP joint through a four-bar linkage mechanism. The MCP and DIP joints rotate relative to each other and do not move independently. This makes the *S-Finger* the finger that has not the shape adaptive feature, [5]. **Fig. 5. A**

The power of the DC motor inside the rigid phalange is transmitted to a pinion via a gearbox with ratio of 1:1024. The power of the pinion is also transmitted by a bevel gearbox with a ratio of 1:2 Face gear, which causes the MCP joint to

rotate, resulting in the movement of the whole artificial finger, [18]. **Fig. 5. B**

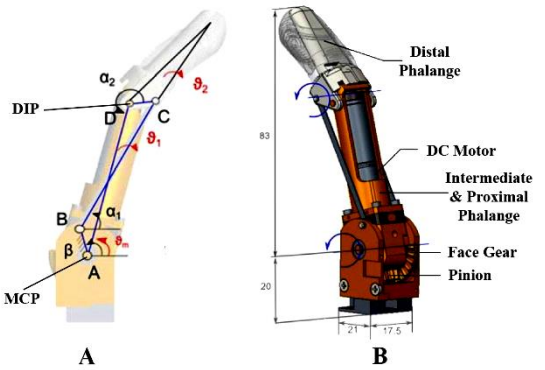

Fig. 5. *S-Finger*: (A) 4-bar linkage mechanism of finger; (B) mechanical design of finger, [18]

The *Southampton* artificial finger is an example of a 2-DOF finger that can be said to be an extended example of the *S-Finger*, [19]. The main difference between *Southampton* and *S-Finger* is that the Intermediate and Proximal phalanges are not rigid and are separated by a PIP joint. Using a Whiffletree mechanism, this artificial finger enables the PIP and DIP joints to move independently of the MCP joint, allowing the proximal and distal joints to move independently of the intermediate joint. The combination of these features makes the *Southampton* finger have both pre-shaping motion and shape adaptive features, [5]. **Fig. 6.**

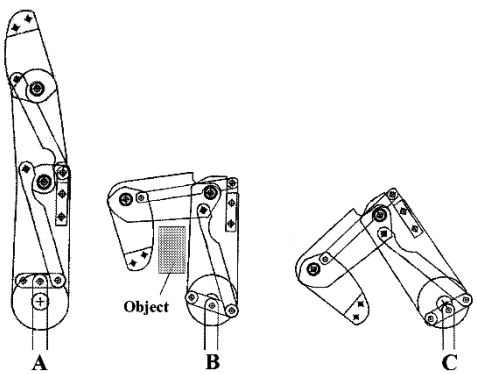

Fig. 6. The *Southampton* prosthetic finger, [19]

The *iLimb* prosthetic finger is another 2-DOF finger that has reached the commercial stage. The general mechanism of this finger is similar to the S-Finger, [11]. There is a fibrous tendon in the DIP joint that allows it to move independently of the MCP joint. This makes the finger shape adaptive, [5]. **Fig. 7.**

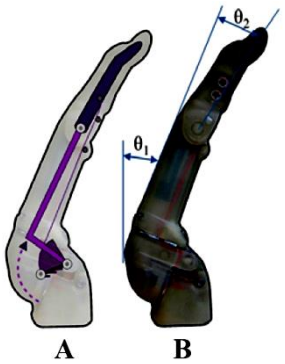

Fig. 7. The iLimb prosthetic finger: (A) mechanism; (B) mechanical design, [11]

The *SARAH* prosthetic finger is a 3-DOF finger made by combining two four-bar linkage mechanisms, [20]. This finger does not have the pre-shaping motion feature because each of the four bar mechanisms does not move independently. But due to its DOFs, it has the shape adaptive feature, [5]. **Fig. 8.**

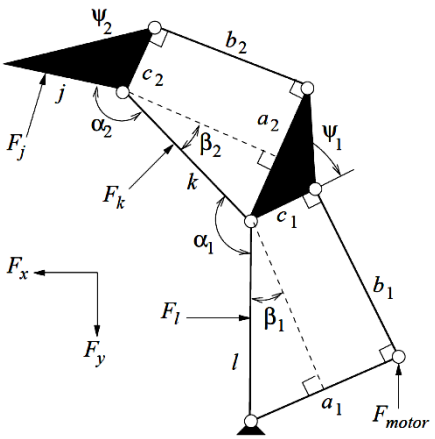

Fig. 8. *SARAH* prosthetic hand, [20]

4. Proposed Design: *ATLAS* Finger

The *ATLAS* prosthetic finger design is inspired by several of designs introduced in previous section. The 4-finger design is actually an extended example of the *S-Finger*, which includes a 4-bar linkage.

By rotating the driver (proximal phalange) around the A (MCP joint), the coupler (BC link) rotates around the B joint, which in turn causes the DC link to rotate around the C (DIP joint), resulting in the distal phalange rotating around the D (DIP joint). **Fig. 9.**

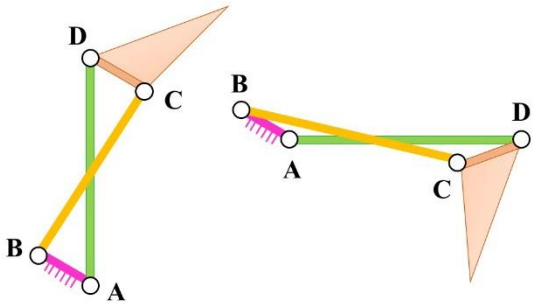

Fig. 9. Kinematic diagram of *ATLAS* 4bar linkage: AB, frame; AD, driver (proximal phalange); BC, coupler; CD, driven (distal phalange)

In the *S-Finger* **Fig. 2** , the motor is located inside the proximal phalange and the coupler link is located outside the finger. In *ATLAS* finger, like the *LISA* finger, the motor is located at the bottom of the MCP joint, and the coupler link is moved into the finger like the *BeBionic* finger, making it look more like a normal human finger. **Fig. 10.**

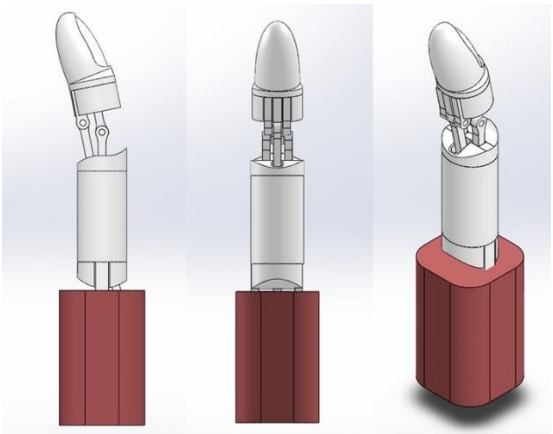

Fig. 10. Index finger of ATLAS

This design is used for the index, middle, ring and little fingers according to the arrangement shown in **Fig. 11.** The axis of symmetry of the middle finger is perpendicular to the palm, but the axis of symmetry of the other fingers has a certain angle to the axis of symmetry of the middle finger. The size of each finger is also according to **Table 1.**

Table. 1. The size of ATLAS hand fingers.

Finger	Index	Middle	Ring	Little
size (mm)	106	111	106	101

The thumb joint has a difficult and complex design because it has 2 DOF. The ATLAS thumb design is inspired by *Galileo* Hand, [14]. In this thumb, the first motor is located inside the metacarpal phalange, which rotates the proximal phalange around the MCP joint, and the second motor is located in the palm of the hand, which can rotate the metacarpal phalange around the CMC joint. **Fig. 12.**

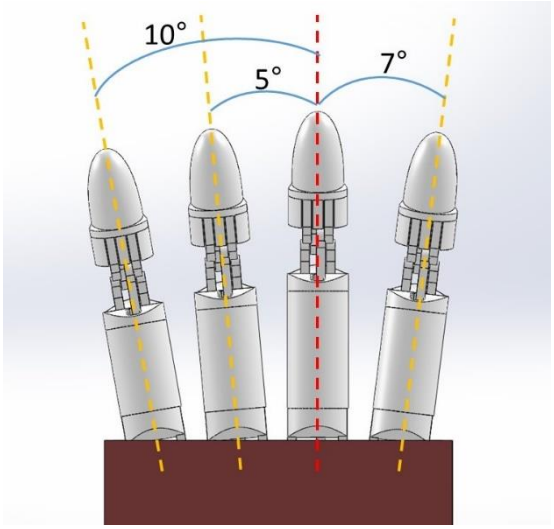

Fig. 11. Palm of ATLAS hand

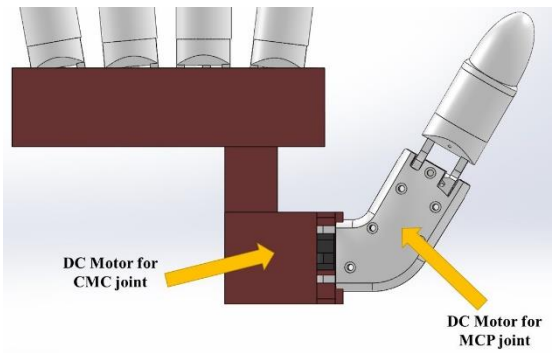

Fig. 12. Thumb finger of ATLAS

To prove the correctness of the design of the ATLAS hand, it is sufficient to compare the amount of distal contact force on one of the natural fingers (for example, the index finger) that is created in contact with an object with the results of the simulated and tested hand.

5. Verification of Design

For verifying the design of fingers and hand, analyzing the contact force of the ATLAS finger, the motion study module of SolidWorks, has been simulated.

A spherical object with a diameter of about 6cm, which is actually a tennis ball, is selected as grasped object. The ball is placed in front of the hand so that if the finger moves, it will make contact with the distal phalange of the index finger. In the simulations, gravity is ignored and the ball is suspended in front of the hand. Since the speed of the DC motor is 200rpm and the power of this motor is transmitted to the MCP joint through a gearbox with ration 1:2, the rotation speed of the MCP joint is 100rpm. Figure 1 shows the simulation process in the form of a stroboscopic photography image of two facing and adjacent views. **Fig. 13.**

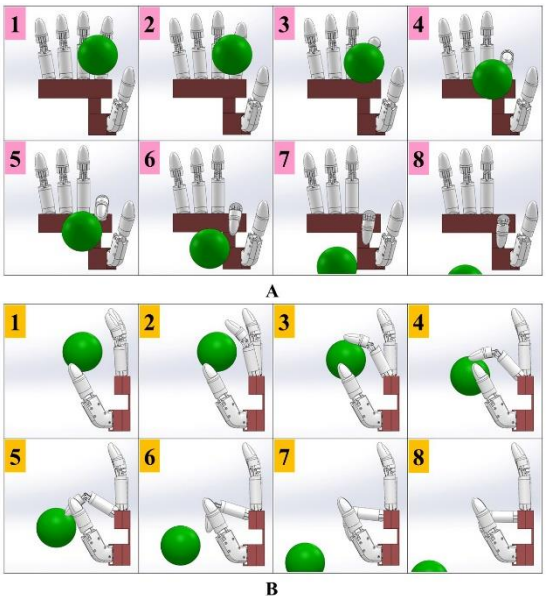

Fig. 13. Stroboscopic photography of the ATLAS hand in grasp process: (A) front view; (B) right view

- **Force Analysis**

Figure 14 shows the distal contact force diagram of the index finger. The red circle indicates the initial moment when the distal phalange hit the ball and the green circle indicates the disconnection of the phalange with the ball. The purple circle also indicates the main moment when the distal phalange hits the ball, when the force reaches its maximum value of 1.6(N).

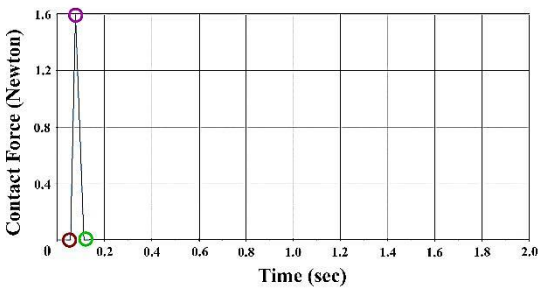

Fig. 14. Contact force between ball and distal phalange of index

- **Motion Analysis**

As shown in the velocity diagram **Fig. 15.** , the angular velocity starts from zero and reaches its grove of 100 rpm. (Green circle) As in **Figure 14**, the red circle indicates the initial moment of impact and the purple circle indicates the maximum contact force between the distal band and the ball.

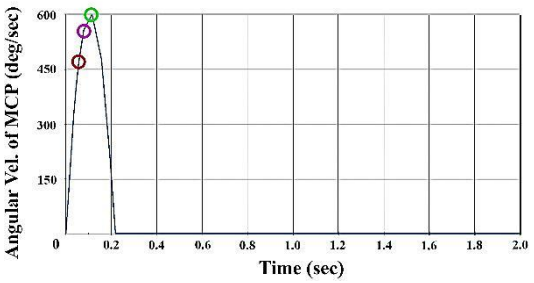

Fig. 15. Angular velocity of MCP joint

Also, by comparing the angular acceleration diagrams of **Figure 16** with the diagrams of **Figures 14 & 15**, we find that at the initial moment of collision (red circle), a sudden increase in angular acceleration occurs, which can be considered as a control impulse. At the moment when the amount of contact force is at its maximum, the acceleration angle is close to zero. (Purple circle) The value is zero at the moment when the Distal contact with the ball is cut off. (Green circle)

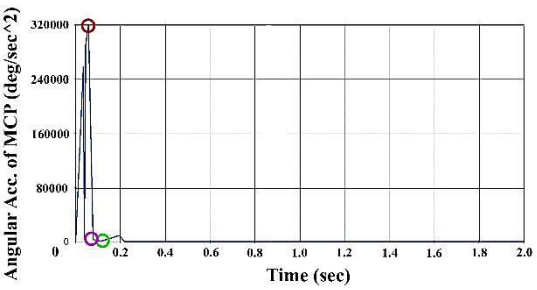

Fig. 16. Angular acceleration of MCP joint

- **Comparison Study: Trajectory Analysis**

To compare the movement path and in fact the working space of The ATLAS finger and the S-Finger design. to place the MCP joint of both fingers at point A and the end points of their distal phalange at point B, with an equal scale, are placing for comparing their path. The path of both fingers is approximately the same but ATLAS takes up less working space than the S-Finger, although this increases its pinching capability. **Fig. 17.**

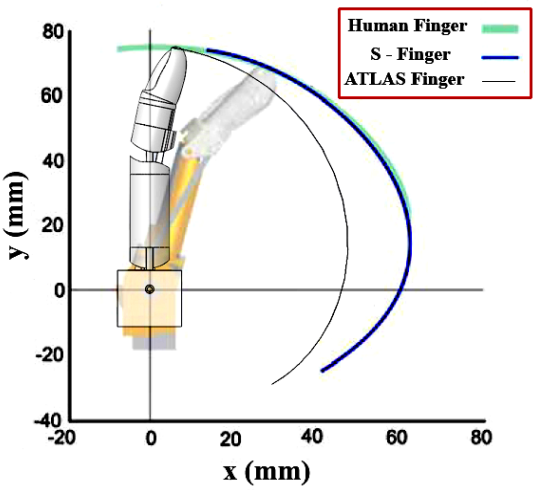

Fig. 17. A comparison between S-Finger[18] and ATLAS finger trajectory

6. Construction

All ATLAS hand pieces are made by *Fused Deposition Modeling* (FDM) 3D-printer with *Polylactic Acid* (PLA) material. Because the production of parts by 3D-printers faces many physical limitations, some parts are printed in several pieces and glued together. **Fig. 18.**

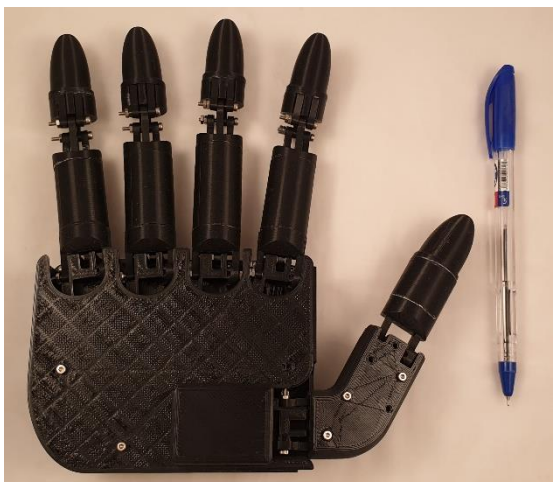

Fig. 18. Overall size of ATLAS Hand

This hand has 6 motors (4 motors for four-finger movement and two motors for thumb movement), which are classified in the group of over actuated hands. DC motors with gearboxes are used to move the ATLAS fingers. The output shaft speed of these motors is 200(rpm). The power of motor is transmitted to the MCP joint via 2 bevel gearboxes with ratio 1:2.

Fig. 19. Overall view of ATLAS Hand

7. Validation of Design: experimental test

In the scientific experiment, we act in accordance with what we did in the simulation. Here we first start the DC motor located on the Index finger with an Arduino board and L298 driver. To obtain contact force, we use an FRS[1] sensor connected to the distal phalange. **Fig. 20.** An FSR is a resistor whose value varies according to the force applied to it. When there is no force, the resistance is infinite, and as the force increases, its value decreases. The amount of force applied to the FSR sensor can be calculated by changing the voltage across the resistor.

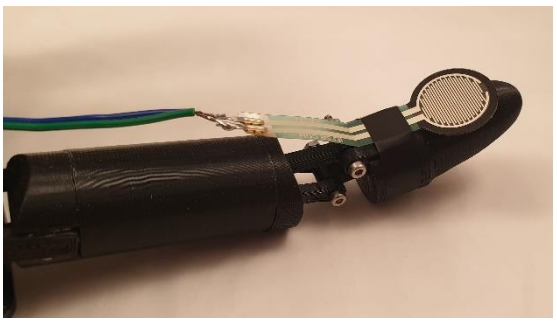

Fig. 20. FSR sensor on Distal phalange on ATLAS

By moving the Index finger and touching the distal phalange with a tennis ball, the output information from the FSR sensor is recorded by the Arduino board. **Fig. 21.** **Fig. 22.** shows the amount of contact force during the test.

Fig. 21. The moment the ATLAS index hits the ball

[1] Force Sensitive Resistor

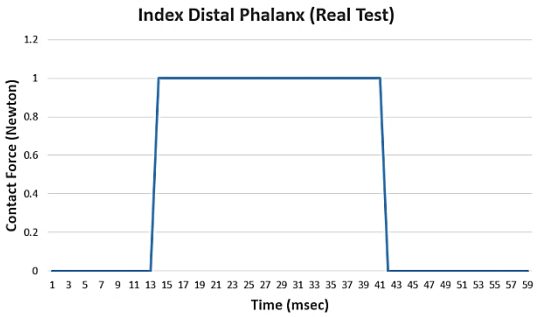

Fig. 22. Contact force in index distal phalange (Real test)

We repeat the same for the natural hand contact force. This time, by connecting the FSR sensor to the distal phalange, we determine the amount of contact force from the Arduino. **Fig. 23&24.**

The amount of force due to the soft contact of the finger with the ball is the same as the hand ATLAS, but with increasing pressure, more force is recorded, which is not to our liking. **Fig. 25.**

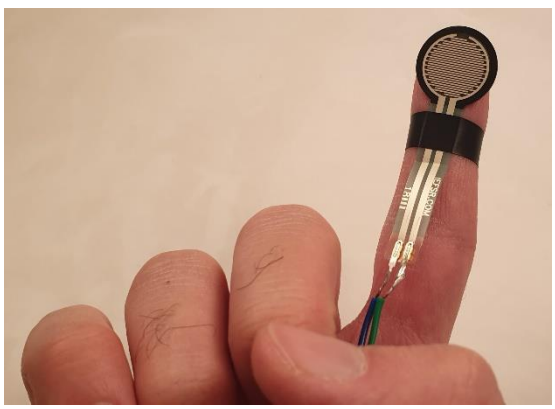

Fig. 23. FSR sensor on distal phalange on natural hand

Fig. 24. The moment the natural hand index hits the ball

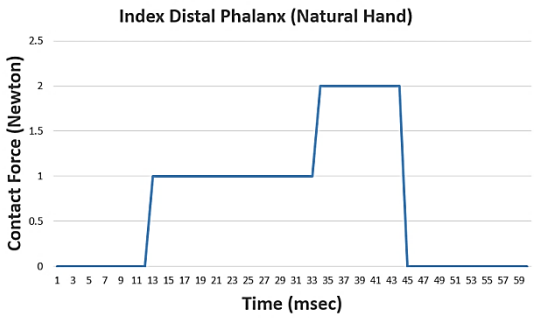

Fig. 25. Contact force in index distal phalange (Natural hand)

Comparing the values of contact force obtained in the simulation, practical experiment and natural hand, it is clear that the ATLAS hand design is optimally close to reality. **Table.2.**

Table. 2. Comparison of contact force

Contact Force	Simulation	Natural Hand	ATLAS Hand
Force (N)	1.3	1	1

8. Conclusion

In this article, we tried to introduce and present the ATLAS artificial finger based on the existing designs. According to the descriptions of the features, operators and mechanism of the artificial fingers, the summary of the ATLAS finger specifications is as shown in **Table 3.**

Table. 3. ATLAS finger specifications

Type	Four bar Linkage-driven
Number of phalanges	2
Number of joints	2
Number of DoF	1
Actuator	1 Geared DC motor
Transmission	Bevel gear 1:2
Shape adaptive	No
Pre shaping motion	No
Manufacturing process	FDM 3D printer
Material	PLA

9. References

[1] A. H. Kermanshahani and F. Cheraghpour Samavati, "Design, Analysis and Control of the 4 Fingers Rehabilitation Robot," (in en), *Journal of Rehabilitation Sciences & Research*, vol. 6, no. 4, pp. 160-168, 2019, doi: 10.30476/jrsr.2019.81926.1021.

[2] E. Difonzo, G. Zappatore, G. Mantriota, and G. Reina, "Advances in Finger and Partial Hand Prosthetic Mechanisms,"

Robotics, vol. 9, no. 4, 2020, doi: 10.3390/robotics9040080.

[3] X. Long and W. Zhang, "A Self-adaptive Robot Finger with a Novel Locking Mechanism for Adjustable Pre-shaping Angle," in *Intelligent Robotics and Applications*, Cham, Z. Chen, A. Mendes, Y. Yan, and S. Chen, Eds., 2018// 2018: Springer International Publishing, pp. 3-15.

[4] "nimblevr." plus.irna.ir/news/83336157/ (accessed.

[5] S. R. Kashef, S. Amini, and A. Akbarzadeh, "Robotic hand: A review on linkage-driven finger mechanisms of prosthetic hands and evaluation of the performance criteria," *Mechanism and Machine Theory*, vol. 145, p. 103677, 2020/03/01/ 2020, doi: https://doi.org/10.1016/j.mechmachtheory.2019.103677.

[6] N. Zainul Azlan and H. Yamaura, "Anthropomorphic finger with optimized geometric parameters for pinching and grasping tasks," *Mechanism and Machine Theory*, vol. 49, pp. 52-66, 2012/03/01/ 2012, doi: https://doi.org/10.1016/j.mechmachtheory.2011.11.005.

[7] F. Cheraghpour, M. Dehghani, A. Feizollahi, P. Sabetian, and S. A. A. Moosavian, "KNTU hand and application of MAG index for form closure grasp," *Journal of the Brazilian Society of Mechanical Sciences and Engineering*, vol. 42, no. 5, p. 267, 2020/04/30 2020, doi: 10.1007/s40430-020-02355-w.

[8] M. T. Leddy and A. M. Dollar, "Preliminary Design and Evaluation of a Single-Actuator Anthropomorphic Prosthetic Hand with Multiple Distinct Grasp Types," in *2018 7th IEEE International Conference on Biomedical Robotics and Biomechatronics (Biorob)*, 26-29 Aug. 2018 2018, pp. 1062-1069, doi: 10.1109/BIOROB.2018.8487198.

[9] P. Wattanasiri, P. Tangpornprasert, and C. Virulsri, "Design of Multi-Grip Patterns Prosthetic Hand With Single Actuator," *IEEE Transactions on Neural Systems and Rehabilitation Engineering*, vol. 26, no. 6, pp. 1188-1198, 2018, doi: 10.1109/TNSRE.2018.2829152.

[10] K. Xu, H. Liu, L. Zenghui, Y. Du, and X. Zhu, "A single-actuator prosthetic hand using a continuum differential mechanism," in *2015 IEEE International Conference on Robotics and Automation (ICRA)*, 26-30 May 2015 2015, pp. 6457-6462, doi: 10.1109/ICRA.2015.7140106.

[11] J. T. Belter, J. L. Segil, and B. SM, "Mechanical design and performance specifications of anthropomorphic prosthetic hands: a review," *Journal of rehabilitation research and development*, vol. 50, no. 5, p. 599, 2013.

[12] P. Sabetian, A. Feizollahi, F. Cheraghpour, and S. A. A. Moosavian, "A compound robotic hand with two under-actuated fingers and a continuous finger," in *2011 IEEE International Symposium on Safety, Security, and Rescue Robotics*, 1-5 Nov. 2011 2011, pp. 238-244, doi: 10.1109/SSRR.2011.6106774.

[13] M. Kamali, S. A. A. Moosavian, and F. Cheraghpour, "Improving grasp capabilities of KNTU hand using position & force sensors," in *2014 22nd Iranian Conference on Electrical Engineering (ICEE)*, 20-22 May 2014 2014, pp. 1278-1283, doi: 10.1109/IranianCEE.2014.6999731.

[14] J. Fajardo, V. Ferman, D. Cardona, G. Maldonado, A. Lemus, and E. Rohmer, "Galileo Hand: An Anthropomorphic and Affordable Upper-Limb Prosthesis," *IEEE Access*, vol. 8, pp. 81365-81377, 2020, doi: 10.1109/ACCESS.2020.2990881.

[15] J. Jin, W. Zhang, Z. Sun, and Q. Chen, "LISA Hand: Indirect self-adaptive robotic hand for robust grasping and simplicity," in *2012 IEEE International Conference on Robotics and Biomimetics (ROBIO)*, 11-14 Dec. 2012 2012, pp. 2393-2398, doi: 10.1109/ROBIO.2012.6491328.

[16] K. Tae-Uk and O. Yonghwan, "Design of spatial adaptive fingered gripper using spherical five-bar mechanism," in *Proceedings of the 2014 International Conference on Advanced Mechatronic Systems*, 10-12 Aug. 2014 2014, pp. 145-150, doi: 10.1109/ICAMechS.2014.6911640.

[17] A. Badawy and R. Alfred, "Myoelectric prosthetic hand with a proprioceptive feedback system," *Journal of King Saud University - Engineering Sciences*, vol. 32, no. 6, pp. 388-395, 2020/09/01/ 2020, doi:

https://doi.org/10.1016/j.jksues.2019.05.002.

[18] I. Imbinto *et al.*, "The S-Finger: A Synergetic Externally Powered Digit With Tactile Sensing and Feedback," *IEEE Transactions on Neural Systems and Rehabilitation Engineering*, vol. 26, no. 6, pp. 1264-1271, 2018, doi: 10.1109/TNSRE.2018.2829183.

[19] P. J. Kyberd, C. Light, P. H. Chappell, J. M. Nightingale, D. Whatley, and M. Evans, "The design of anthropomorphic prosthetic hands: A study of the Southampton Hand," *Robotica*, vol. 19, no. 6, pp. 593-600, 2001, doi: 10.1017/S0263574701003538.

[20] T. Laliberté and C. M. Gosselin, "Underactuation in space robotic hands," in *Proceeding of the Sixth International Symposium on Artificial Intelligence, Robotics and Automation in Space ISAIRAS: A New Space Odyssey*, 2001.

Biography

Aryan Gorjestani received his BSc. degree in Mechanical Engineering from the Pardis Science & Technology branch of Islamic Azad University, Tehran, Iran in 2017, and his MSc. degree from the Pardis Science & Technology branch of Islamic Azad University, Tehran, Iran in2021. His research interests include Dynamics, Control and Robotics, especially bionic and rehabilitation systems.

Farzad Cheraghpour Samavati is currently an assistant professor in the faculty of Mechanical Engineering at Pardis Science & Technology branch of Islamic Azad University, Tehran, Iran. He received his MSc. and Ph.D. degrees in Mechanical Engineering from K. N. Toosi University of Technology in 2006 and 2013 respectively. His research interests include grasp planning of robotic systems and assistive robotics.